Available online at www.sciencedirect.com
SCIENCE DIRECT
Journal of Magnetic Resonance 180 (2006) 72–82
JMR Journal of Magnetic Resonance
www.elsevier.com/locate/jmr

Resolution enhancement in spectra of natural products dissolved in weakly orienting media with the help of ^{1}H homonuclear dipolar decoupling during acquisition: Application to ^{1}H–^{13}C dipolar couplings measurements

Jonathan Farjon [a], Wolfgang Bermel [b], Christian Griesinger [a,*]

[a] Max Planck Institut für Biophysikalische Chemie, Abt. 030, Am Faßberg 11, 37077 Göttingen, Germany
[b] Bruker Biospin GmbH, Silberstreifen 4, 76287 Rheinstetten, Germany

Received 27 July 2005; revised 3 January 2006
Available online 13 March 2006

Abstract

In weakly orienting media such as poly-γ-benzyl-L-glutamate (PBLG) a polymer that forms a chiral liquid crystal in organic solvents, the spectral resolution for embedded molecules is usually poor because of numerous ^{1}H, ^{1}H dipolar couplings that generally broaden proton spectra. Therefore ^{1}H, ^{13}C dipolar couplings are difficult or impossible to measure. Here, we incorporate Flip-Flop decoupling during detection into an HSQC experiment. Flip-Flop removes the ^{1}H, ^{1}H dipolar couplings and scales the chemical shifts of the protons as well as the ^{1}H, ^{13}C dipolar couplings during detection. A resolution gain by a factor 1.5–4.2 and improved signal intensity by an average factor of 1.6–1.7 have been obtained. This technique is demonstrated on (+)-menthol dissolved in a PBLG/$CDCl_3$ phase.

Keywords: Homonuclear dipolar decoupling; Spectral resolution; Sensitivity; PBLG; Dipolar couplings; Natural products

1. Introduction

The determination of the stereochemistry of compounds that have for example been isolated and need to be characterized for the first time is an important challenge in chemistry and in pharmaceutical industries. While the conventional NMR parameters like NOE and *J*-coupling constants provide informations about the configuration in rigid compounds, this is difficult or impossible in cases where the molecule is flexible or the stereocenters are distant in the bonding network. It has recently been shown by several groups that dipolar couplings measured for organic molecules in orienting media are not only useful for structure determination of biomolecules [1] but also very promising for solving stereochemical problems [2]. The anisotropic solvents are chiral nematic liquid crystalline phases in the presence of a magnetic field. They are composed of homopolypeptides such as poly-γ-benzyl-L-glutamate (PBLG) [3], poly-γ-ethyl-L-glutamate (PELG) and poly-ε-carbobenzyloxy-L-lysine (PCBLL) [4] in mixture with organic solvents.

These phases align molecules more strongly than water compatible orienting media usually employed for biomolecules. Therefore, they not only render large heteronuclear dipolar couplings between nuclei that are directly bound to one another but also large ^{1}H, ^{1}H dipolar couplings that usually make the proton spectra undecipherable (Fig. 1). Consequently ^{1}H, ^{13}C dipolar couplings are difficult and inaccurately or even impossible to measure. These problems are aggravated the more protons the studied molecule has. Since for the mentioned chiral orienting media the alignment cannot be reduced below a given value by dilution it is highly desirable to remove the ^{1}H, ^{1}H dipolar

* Corresponding author. Fax: +49 551 201 2202.
E-mail address: cigr@nmr.mpibpc.mpg.de (C. Griesinger).

1090-7807/$ - see front matter © 2006 Elsevier Inc. All rights reserved.
doi:10.1016/j.jmr.2006.01.006

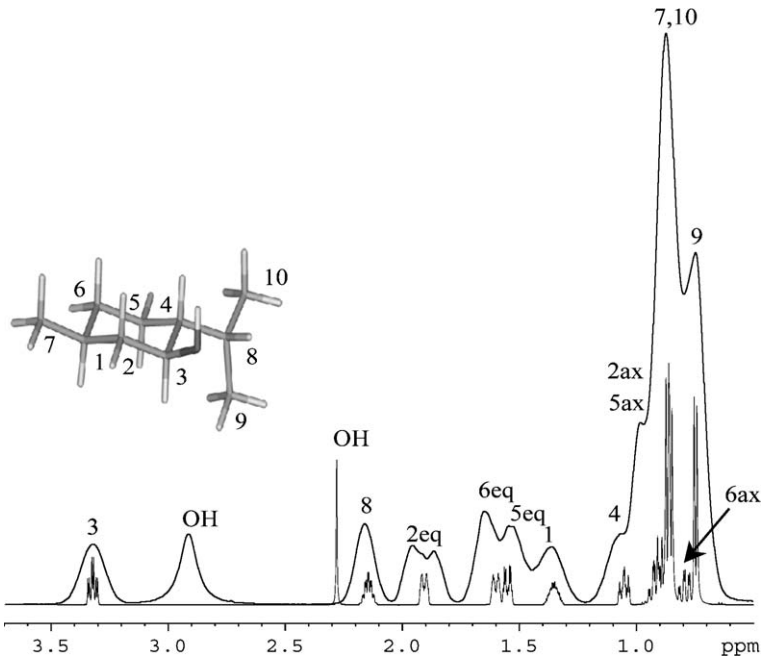

Fig. 1. Superimposition of ^{1}H signals of (+)-menthol in $CDCl_3$ and PBLG/$CDCl_3$ (signals in bold) and its molecular structure as well as the used numbering.

couplings and at the same time retain the desired heteronuclear couplings.

Various methods have been used to reduce or eliminate anisotropic interactions in solid-state NMR to decrease the linewidths of the NMR peaks. For $I = 1/2$ spin systems the line-broadening is mainly due to dipolar couplings. Techniques to reduce the linewidth like magic angle sample spinning, homonuclear dipolar decoupling, and broadband heteronuclear decoupling were intensively used. One of the first methods of homonuclear dipolar decoupling was off-resonance continuous wave (CW) irradiation, introduced by Lee and Goldburg [5]. Later, Waugh et al. [6] introduced the multiple-pulse WAHUHA sequence to remove the dipolar terms in the average spin Hamiltonian up to the first-order to achieve more efficient decoupling of homonuclear dipolar couplings. Then, many other multiple-pulse dipolar decoupling sequences have been proposed for further improvement. In particular, one of the most used methods is the 8-pulse MREV-8 sequence [7]. The combination of magic angle sample spinning and multiple pulse dipolar decoupling CRAMPS [8] has proven to be very useful for obtaining high-resolution proton spectra of solids. Then longer multiple pulse sequences were used to improve the ^{1}H, ^{1}H decoupling: BR-24 [9] and BLEW-48 [10] have been developed and used for homonuclear dipolar decoupling to study liquid crystals [11]. In 1989, Levitt and co-workers [12] demonstrated that the magic-angle CW method of Lee and Goldburg [5] could be improved by frequency switching. Very recently Grzesiek and co-workers [13] used INEPT- or HMQC-type experiments including frequency switched Lee–Goldburg sequence to reduce ^{1}H, ^{1}H dipolar couplings and detect small heteronuclear dipolar couplings. However, these multiple pulse sequences are windowless or have only small delays without irradiation and therefore are not feasible for homonuclear decoupling during detection.

Ten years ago, Ouvrard et al., introduced the Flip-Flop 16 (FF16) sequence (see Fig. 2) made of 16 pulses into the t_1 evolution time of COSY experiment. FF16 was used for turning second-order spectra into first-order spectra obtained for small organic molecules dissolved in thermotropic media [14].

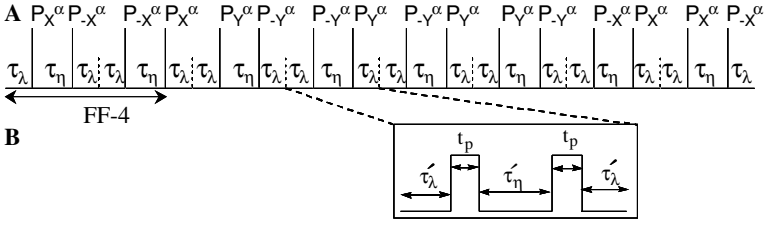

Fig. 2. (A) Schematic representation of the FF16 and FF4 sequence. $P_\varphi\alpha$ indicates a pulse with flip angle α and phase φ. (B) Expansion of a two pulse subcycle of the FF16 sequence in which the finite pulse width t_p is taken into account. τ'_λ and τ'_η are variable delays of the sequence.

In the literature, further methods to reduce homonuclear dipolar couplings have been proposed. Courtieu et al. [15] introduced the variable angle sample spinning (VASS) technique that has been recently used also by Thiele [16]. Selective pulses permitted to highly simplify ^{1}H and ^{13}C spectra of various mixtures of enantiomers dissolved in PBLG phases by using SERF [17] and HETSERF [18] experiments. Band selective decoupling was used to decouple selectively some regions of ^{1}H [19] or ^{13}C spectra [20] for enhancing the spectral resolution. Other methods based on the utilization of BIRD sequences allow the efficient removal of long range ^{1}H, ^{13}C dipolar couplings for measuring direct couplings [21].

To overcome the line-broadening problem in PBLG phases during proton detection, we were interested in efficient sensitive techniques that are not limited by the type of orienting medium or that required specific non-standard hardware like the VASS technique [15]. Thus, multiple pulse sequences with short times of rf-irradiation and long delays to allow for recording the signal have been chosen to obtain an overall good sensitivity of detection. To this goal, in this paper we demonstrate that an HSQC with Flip Flop (FF) decoupling during t_2 (HSQC-FF) in particular using a four-step supercycle (FF4) provides the necessary resolution enhancement to easily measure dipolar couplings without loss of sensitivity. The potential of the method will be illustrated on (+)-menthol dissolved in a PBLG/$CDCl_3$ phase.

2. Theory

We have chosen the multiple pulse sequences FF for homonuclear decoupling since it has two advantages in comparison with other multiple pulse sequences. On the one hand, by design, miscalibration of pulses is self-compensated since a pulse with flip angle α is followed by a pulse with flip angle $-\alpha$ [22] (Fig. 2). On the other hand due to the limited number and duration of the pulses, long delays can be used for detection as opposed to other sequences that have smaller windows. The spin Hamiltonians in frequency units (division by Planck's h) at zeroth order of a weakly aligned molecule under an FF sequence can be represented by

$$\overline{H}^{(0)}_{\mathrm{FF}} = K_{\mathrm{CS}}(H_{Z_{\mathrm{H}}} + H_{T_{\mathrm{CH}}}) + K_{\mathrm{D}}H_{D_{\mathrm{HH}}} + H_{J_{\mathrm{HH}}} + H_{Z_{\mathrm{C}}} + H_{T_{\mathrm{CC}}}. \quad (1)$$

$H_{Z_{\mathrm{H}}}$ and $H_{Z_{\mathrm{C}}}$ are the Zeeman interaction terms for ^{1}H and ^{13}C, respectively, thus

$$H_{Z_{\mathrm{H}}} = -\sum_i v_i^{\mathrm{H}} I_{iz},$$

$$H_{Z_{\mathrm{C}}} = -\sum_i v_i^{\mathrm{C}} \mathrm{S}_{iz},$$

where I_{iz} and S_{iz} are the component of the nuclear spin angular momentum operators along the z-axis for ^{1}H and ^{13}C, respectively. In Eq. (1), $H_{T_{\mathrm{CH}}}$ and $H_{T_{\mathrm{CC}}}$ are the total spin–spin coupling terms that include both dipolar and scalar couplings:

$$H_{T_{\mathrm{CH}}} = \sum_{i<j} T_{ij}^{\mathrm{CH}} I_{iz} S_{jz} = \sum_{i<j} \left(D_{ij}^{\mathrm{CH}} + J_{ij}^{\mathrm{CH}}\right) I_{iz} S_{jz},$$

$$H_{T_{\mathrm{CC}}} = \sum_{i<j} T_{ij}^{\mathrm{CC}} S_{iz} S_{jz} + \frac{1}{2}\left(J_{ij}^{\mathrm{CC}} - \frac{D_{ij}^{\mathrm{CC}}}{2}\right)\left(S_i^{+} S_j^{-} + S_i^{-} S_j^{+}\right),$$

where $T_{ij} = D_{ij} + J_{ij}$. D_{ij} and J_{ij} are the dipolar and scalar coupling constants, respectively. The two terms $H_{J_{\mathrm{HH}}}$ and $H_{D_{\mathrm{HH}}}$ are

$$H_{J_{\mathrm{HH}}} = \sum_{i<j} J_{ij}^{\mathrm{HH}} I_{iz} I_{jz} + \frac{J_{ij}^{\mathrm{HH}}}{2}\left(I_i^{+} I_j^{-} + I_i^{-} I_j^{+}\right),$$

$$H_{D_{\mathrm{HH}}} = \sum_{i<j} D_{ij}^{\mathrm{HH}} I_{iz} I_{jz} - \frac{D_{ij}^{\mathrm{HH}}}{4}\left(I_i^{+} I_j^{-} + I_i^{-} I_j^{+}\right).$$

While the J_{ij}^{HH} due to its isotropic nature is not affected by the homonuclear decoupling sequence, the dipolar homonuclear coupling D_{ij}^{HH} is scaled by the expression:

$$K_{\mathrm{D}} = 1 - \frac{3(\tau'_\eta + t_p)}{2(2\tau'_\lambda + \tau'_\eta + 2t_p)} \sin^2 \alpha. \quad (2)$$

The proton chemical shift and similarly the heteronuclear J_{ij}^{CH} and D_{ij}^{CH} and therefore also the total coupling $T_{ij}^{\mathrm{CH}} = J_{ij}^{\mathrm{CH}} + D_{ij}^{\mathrm{CH}}$ are scaled by the factor K_{CS}:

$$K_{\mathrm{CS}} = \frac{2\tau'_\lambda + \tau'_\eta(\cos\alpha) + t_p(1+\cos\alpha)}{(2\tau'_\lambda + \tau'_\eta + 2t_p)}. \quad (3)$$

Both scaling factors K_{CS} and K_{D} depend on the delays and flip angle of the sequence.

We will see that with the help of Eq. (1) one bond distance dipolar C, H couplings could be deduced experimentally from the scaled total couplings: $T_{ij}^{\mathrm{CH,red}} = K_{\mathrm{CS}} T_{ij}^{\mathrm{CH}}$ and the scalar ^{13}C, ^{1}H coupling $^{1}J_{\mathrm{CH}}$ by the following equation:

$$^{1}D_{ij}^{\mathrm{CH}} = \frac{^{1}T_{ij}^{\mathrm{CH,red}}}{K_{\mathrm{CS}}} - {}^{1}J_{ij}^{\mathrm{CH}}. \quad (4)$$

Eqs. (2) and (3) can be further simplified to design the FF sequence with optimal decoupling properties and optimal signal. For complete removal of the ^{1}H, ^{1}H dipolar couplings, we set K_{D} to 0. Furthermore, the total duration of the FF cycle is the dwell time (dw) whose inverse corresponds the desired spectral width. Then, K_{CS} can be expressed in term of one variable, namely the flip angle α of the FF sequence (see Fig. 3A):

$$K_{\mathrm{CS}} = 1 + \frac{2}{3}\sin^{-2}\alpha(\cos\alpha - 1) \text{ with}$$

$$\tau'_\eta = \left(\frac{2}{3}\sin^{-2}\alpha - \frac{\mathrm{DR}}{2}\right)\mathrm{dw} \text{ and } 2\tau'_\lambda = (1-\mathrm{DR})\mathrm{dw} - \tau'_\eta.$$

Another variable that determines the amount of signal to be detected is the ratio between the times that the receiver is open and the total duration of acquisition. During the α-pulses and some dead time before and after the pulse the

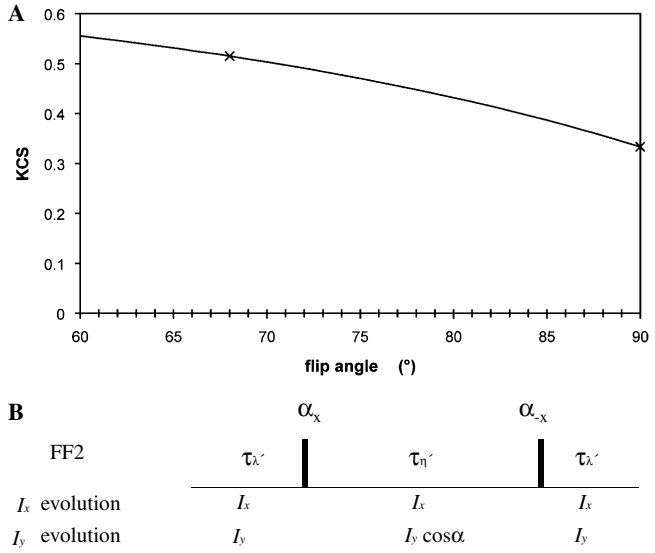

Fig. 3. (A) Correlation between the scaling factors K_{CS} and the flip angle α for $K_D = 0$. The smallest usable flip angle was 68° for practical reasons, since t'_λ should be bigger than 3.9 μs because of dead times to open and close the receiver. $dw = 2\tau'_\lambda + \tau'_\eta + 2t_p$ is equal to 104.8 μs. Crosses indicate the experimentally used conditions. (B) Evolution of transverse proton coherences during the FF2 unity block.

receiver must be shut. While for maximum signal the receiver should be open as long as possible, this would require minimum dead times DT and minimum duty ratio DR which in turn requires high power for the pulses. Thus, there is a limitation that the probe and the receiver circuitry imposes, namely to have an average power during detection that is still compatible with the probe and dead times that avoid artefacts in the spectrum from pulse ring down.

In the following, we calculate the signal that can be expected from detection during which a Flip-Flop sequence is applied. Theoretically, due to shorter times during which the receiver is open, the noise will be reduced to $\sqrt{1 - DR - DT}$ and the signal by a factor of $1 - DR - DT$ and therefore by calculation of the signal we also can calculate the signal to noise ratio. However, it turned out that the noise in FF decoupled spectra is not random. The fact that the noise is not random does not pose a problem since the non-randomness of the noise does not increase the noise amplitude too much. The signals are still much stronger than the noise even with the non-white contributions. Therefore, we compare only the signal, easily distinguishable from the noise, to assess the efficiency of FF with respect to detection without FF decoupling. Signal comparison can only and reliably be done with the same hardware conditions: the same acquisition mode: in our case QSIM, the same digital mode: Analog and with an external analog filter.

While Eqs. (2) and (3) are sufficient to optimise the decoupling performance for FF sequences applied in evolution times, the scaling factor of the signal (K_S) must be taken into account. It originates from the fact that the detectable proton coherences I_x and I_y evolve differently during the FF2 scheme and that the receiver is open only during the windows (i.e., $2\tau'_\lambda + \tau'_\eta$) of the decoupling sequence. By convention, the detectable proton coherence is $I^- = I_x - iI_y$ with I_x and I_y the transverse proton coherences along x and y-axis, respectively. By assuming the "on resonance" case during an FF2 unity block, I_x does not change during the delays, however I_y is reduced to $I_y \cos\alpha$ during τ'_η (see Fig. 3B). From this we obtain by calculating the amplitude of I^- during one FF2-cycle the scaling factor K_S for the signal:

$$K_S = E \times \sqrt{\left(\frac{2\tau'_\lambda + \tau'_\eta - DT}{2\tau'_\lambda + \tau'_\eta + 2t_p}\right)^2 + \left(\frac{2\tau'_\lambda + \tau'_\eta \cos\alpha - DT}{2\tau'_\lambda + \tau'_\eta + 2t_p}\right)^2}, \quad (5)$$

E is a factor, that reflects the intrinsic efficiency of the FF decoupling for reducing the linewidth and is a complicated function of the dipolar as well as scalar couplings that are present in the multiplet under investigation. K_S is the same irrespective of the cycle number of the FF sequence (FF2, FF4, FF8, or FF16).

To describe the efficiency of the decoupling, we will use also a dispersion ratio that reflects the reduction in linewidth (reflected also in the E factor) that is partially offset by the reduction of the chemical shift by the factor K_{CS}. The relative proton linewidth of the reference Γ_0 and FF spectra Γ_{FF} and the differences in chemical shifts between two resonances in the standard $\Delta\nu_0$ and the FF spectrum $\Delta\nu_{FF}$ can be used to calculate the dispersion factor $K_{dispersion}$:

$$\frac{\Delta\nu_{FF}}{\Gamma_{FF}} \Big/ \frac{\Delta\nu_0}{\Gamma_0} = \frac{\Gamma_0}{\Gamma_{FF}} K_{CS} = K_{dispersion} \quad (6)$$

$K_{dispersion}$ is the larger the narrower the proton multiplet becomes under FF decoupling and the less the chemical shift is scaled due to the decoupling. Thus a large $K_{dispersion}$ is desirable. In the following resolution and dispersion will be discussed and the dispersion is the most interesting to evaluate the FF efficiency.

3. Results and discussion

For evaluating the potential of Flip-Flop experiments inserted during the acquisition time, (+)-menthol has been dissolved in PBLG/$CDCl_3$. First, the FF16 sequence has been implemented during the acquisition time of a standard 1D 90° pulse experiment. However, strong artifacts are observed in the FF16 spectra (Figs. 4A and C) that may even overlap with signals of the molecule. In Figs. 4B and D, a considerable reduction of the number of artifacts can be seen with FF4, which is the first fourth of the FF16 cycle (Fig. 2A). By comparison to the standard proton spectrum a clear resolution enhancement is observed (Fig. 5). In the standard 1D proton spectrum (Fig. 5A) of (+)-menthol in PBLG/$CDCl_3$, the proton signal of the proton 2 equatorial

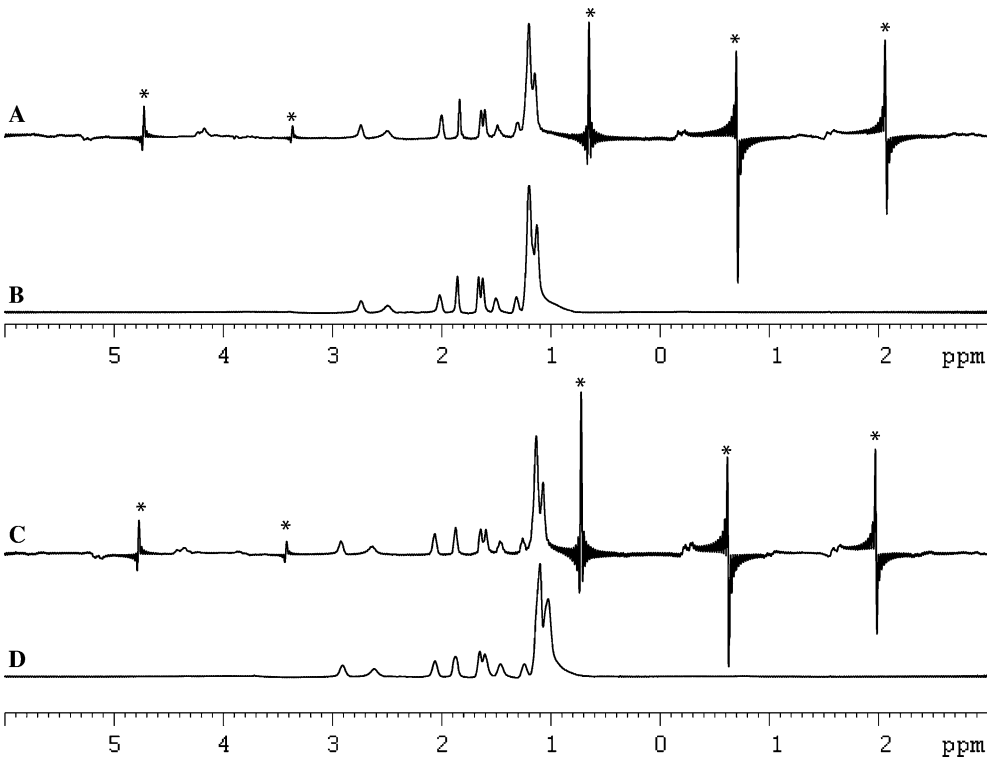

Fig. 4. Comparison between 1D FF proton spectra for different flip angles for menthol in PBLG/$CDCl_3$ phase. FF16 with 90° (A) and 68° (C) flip angle. FF4 with 90° (B) and 68° (D) flip angle. *Artefacts due to the FF16 sequence.

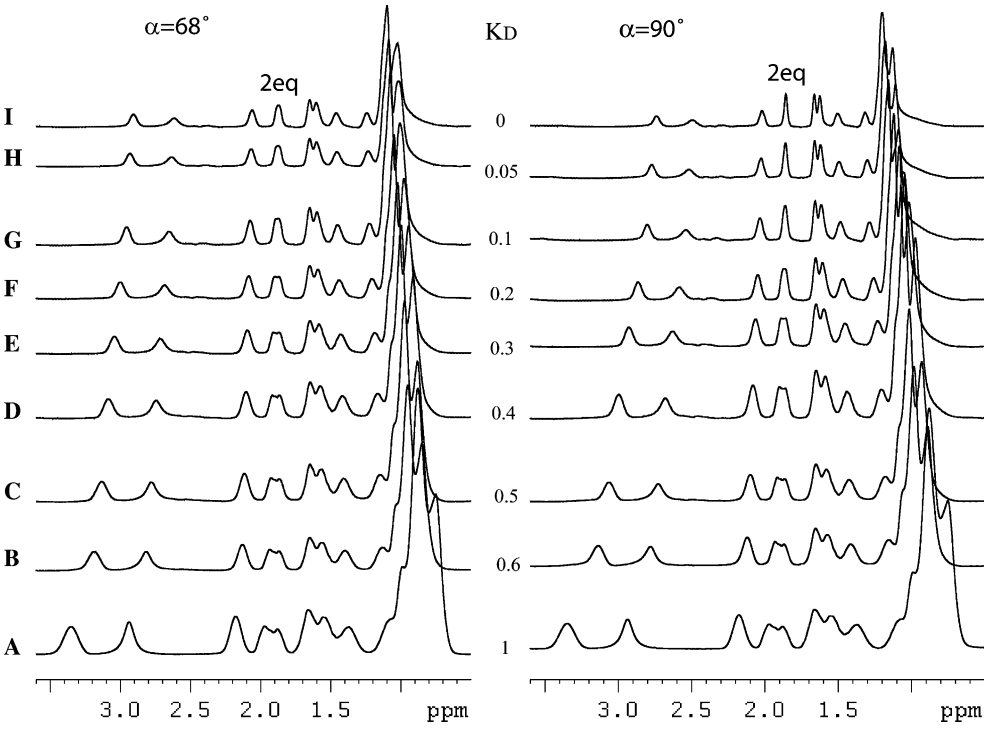

Fig. 5. Series of proton 1D spectra. (A) Standard 1D without FF4 sequence. From (B) to (I) are 1D spectra with FF4 during acquisition with decreasing K_D value with different flip angles (mentioned above each spectrum). For each spectrum, 8 scans and a recycle delay of 2s and a carrier set at 1.23 ppm have been used.

(2eq) is a broad doublet due to the total spin–spin coupling $T^{HH}_{2ax,2eq}$ between the geminal protons 2eq and 2ax. With FF4 decoupling during acquisition, this splitting is reduced and undetectable already for $K_D = 0.2$. Further reduction of K_D to 0 reduces the line width of the singlet even further. The experimental values of K_D derived from $T^{HH}_{2ax,2eq}$ measure-

ments on spectra 5B ($K_D = 0.6$) to 5E ($K_D = 0.3$) are close to the expected value, the relative error is less than 5% on the 2eq signal. In the reference 1D spectrum (Fig. 5A) for the region 1–1.7 ppm, resonances are poorly resolved, however in the FF4 spectra (Fig. 5I, $K_D = 0$) each resonance is resolved due to the resolution gain of the FF4 sequence even if the dispersion of the chemical shifts is reduced by $K_{CS} = 0.51$ for $\alpha = 68°$ and by $K_{CS} = 0.33$ for $\alpha = 90°$. The reduction of the linewidth is clearly observed for several proton multiplets in Fig. 6 when K_D decreases, as expected. For $K_D = 0$ and a flip angle of 68° or 90°, most of the protons of menthol are well dispersed, which permits to measure direct ^1H, ^{13}C dipolar couplings simply by inspection and with a better accuracy than without FF4 decoupling.

To this aim, the FF4 sequence has been implemented during acquisition of an HSQC experiment during the detection (see Section 5). This experiment has been applied on (+)-menthol in PBLG/$CDCl_3$. In Fig. 7, HSQC traces of a standard HSQC and an HSQC-FF4 can be compared. As an example the ω_2-trace for the H_5 protons extracted from the standard HSQC spectrum shows a very broad multiplet and the heteronuclear coupling cannot accurately be extracted. By comparison, the ω_2-trace through the H_5 resonance extracted from the HSQC-FF4 spectra shows two narrow doublets one for each geminal proton due to the reduced total coupling between each of them and the carbon C_5: $K_{CS}T^{CH}_{H5ax,C5}$ and $K_{CS}T^{CH}_{H5eq,C5}$. The efficiency of FF4 decoupling can also be appreciated on the ω_2-trace

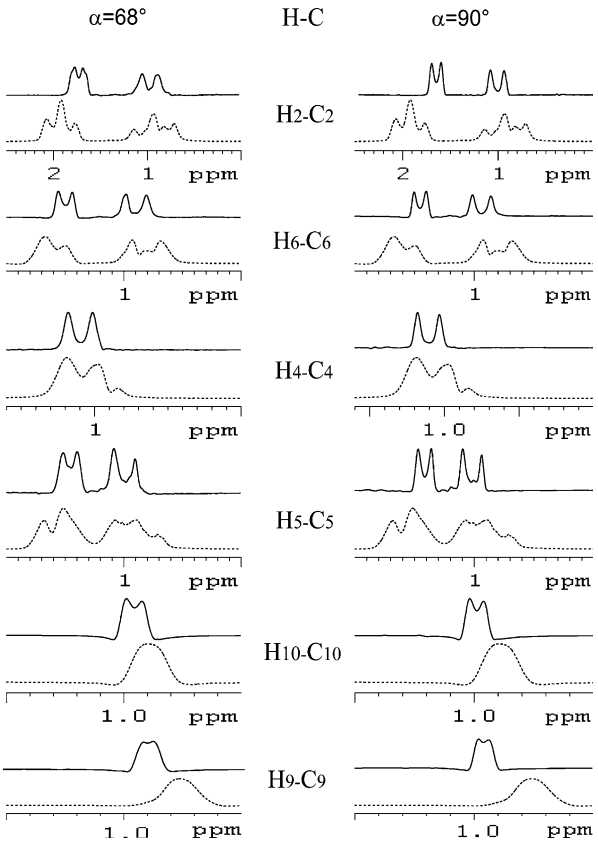

Fig. 7. Extracted F_2 traces from ^1H, ^{13}C HSQC-FF4 spectra and HSQC spectra (dotted lines). The carrier is set to 1.23 ppm. Flip angles are indicated above each spectrum.

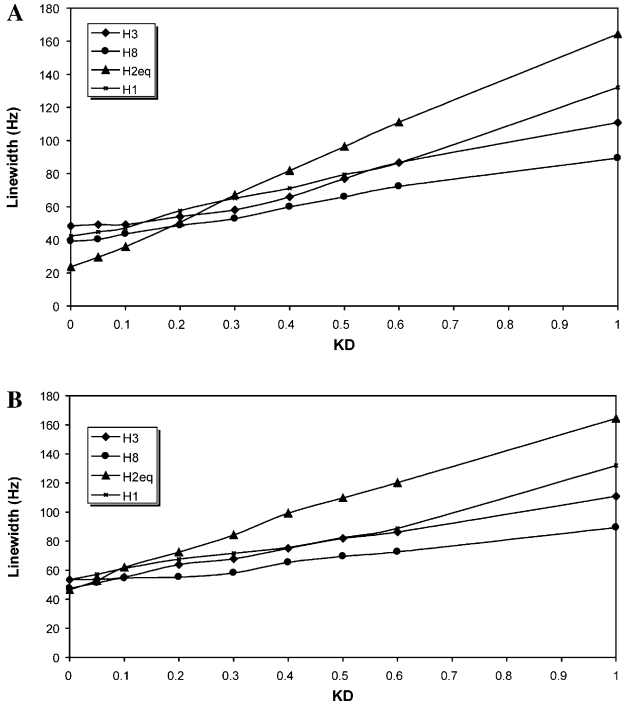

Fig. 6. Graphical representation of the linewidth of some protons of (+)-menthol in PBLG/$CDCl_3$ relative to the value of the scaling factor K_D. (A) $\alpha = 90°$, (B) $\alpha = 68°$.

of the protons H_9 and H_{10}: where the $K_{CS}T^{CH}_{Me9,C9}$ and $K_{CS}T^{CH}_{Me10,C10}$ can be extracted from the FF4 spectrum.

By quantitative analysis we find that the HSQC-FF4 increases resolution by a factor of 1.5–4.2 (see Fig. 8A). We observe better resolution as well as a gain in sensitivity for methylenes 2, 5, and 6 but also for methines 1 and 4, since they are coupled with numerous protons of the ring as well as for methyls 9 and 10 that are mutually coupled by a ^1H, ^1H dipolar coupling. However, the reduction in linewidth and consequently increase in signal amplitude is for some proton signals overcompensated by the signal loss due to the reduction of the duty cycle of the receiver. This can be observed especially for those protons where only a few dipolar couplings broaden the lines in the conventional experiment and where the linewidth increase is therefore smaller than for those protons that have a large number of dipolar couplings. The former is true for example for protons 7 and 8.

In Fig. 8B, the dispersion ratio $K_{dispersion}$ as defined in Eq. (6) is shown. Firstly, we find the dispersion ratio to be bigger than 1 for $\alpha = 68°$ by some margin for all resonances except for two (see Fig. 8B) indicating that reduction of the chemical shifts is offset by the reduction in the linewidth. The pulse sequence using the flip angle $\alpha = 68°$ performs slightly better than the one using 90°. This is most

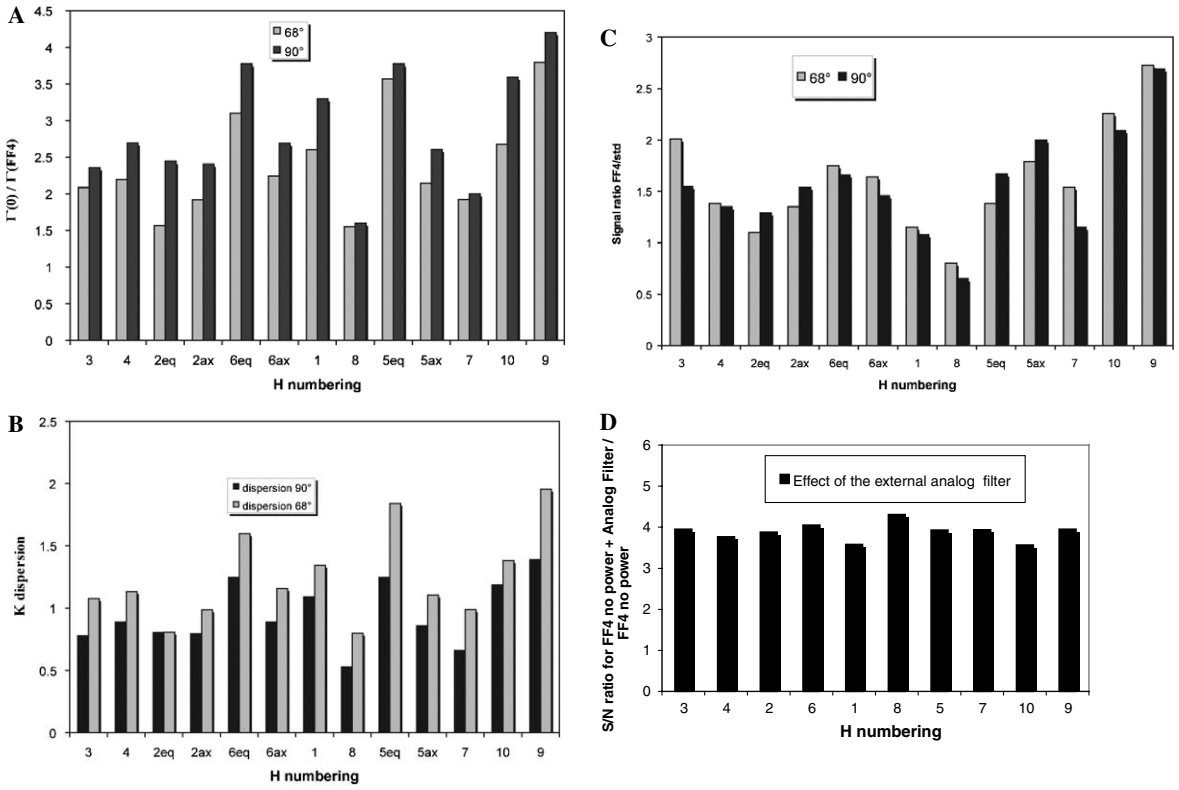

Fig. 8. (A) Linewidth ratio between standard HSQC and HSQC-FF4 spectra for the numbered protons of (+)-menthol. (B) Dispersion ratio (see text) between standard HSQC and HSQC-FF4 spectra for numbered protons of (+)-menthol. (C) Signal ratio between HSQC-FF4 spectra and standard HSQC spectra for numbered protons of (+)-menthol. QSIM acquisition mode with an external analog filter (in black $\alpha = 90°$) and grey ($\alpha = 68°$). (D) External analog filter effect (for $\alpha = 90°$) was evaluated from comparing the S/N ratio between FF4 spectra with no power in the FF pulses recorded by using a external analog filter and FF4 spectra with no power in the FF pulses.

Table 1
FF4 acquisition parameters for different flip angles

	Flip angle (°)	
	68	90
dw (μs)	104.8	104.8
K_D	0	0
K_{CS}	0.51	0.33
K_S^{th} [a]	0.66	0.53
K_S^{exp} [b]	0.63	0.50
t_p (μs)	14.79	19.57
τ'_λ(μs)	4.37	7.68
τ'_η(μs)	66.49	50.3
DR	0.28	0.37

[a] Theoretical K_S.
[b] Experimental K_S.

Table 2
Relative signal intensity between HSQC-FF4 and standard HSQC experiments

Proton	Flip angle [a] (°)	
	90 FF4/std AF[b]	68
H3	1.55	2.01
H4	1.35	1.38
H2eq	1.29	1.10
H2ax	1.54	1.35
H6eq	1.66	1.75
H6ax	1.46	1.64
H1	1.08	1.15
H8	0.65	0.80
H5eq	1.67	1.38
H5ax	2.00	1.79
H7	1.15	1.54
H10	2.09	2.26
H9	3.34	4.01
Average value	1.60	1.70

[a] Flip angle used in degree in the FF4 sequence.
[b] An external analog filter (AF) was used to record the standard and the FF4 experiment.

probably due to the bigger $K_{CS} = 0.51$ for $\alpha = 68°$ instead of $K_{CS} = 0.33$ for $\alpha = 90°$ (Table 1).

FF decoupling also improves the signal intensity by an average factor of 1.6 for $\alpha = 90°$ and 1.7 and $\alpha = 68°$ (see Fig. 8C and Table 2) compared to the standard HSQC spectrum by using an external analog filter. The efficiency factor E of the FF4 sequence can be deduced from Eq. (5) and was found to be on average close to 3 for flip angles 68° and 90° (Table 3).

K_{CS} values have been experimentally obtained (K_{CS}^{exp}) from each proton chemical shifts [see Eq. (1)] in standard and FF spectra. K_{CS}^{exp} values only weakly differ from the the-

Table 3
Ratio of signal-to-noise ratios of powerless HSQC-FF4 with and without external analog filter

Proton	S/N ratio[a]
H3	3.95
H4	3.77
H2	3.88
H6	4.05
H1	3.58
H8	4.31
H5	3.93
H7	3.94
H10	3.57
H9	3.95
Average value	3.89

[a] The signal to noise ratio between HSQC-FF4 recorded with no power for FF sequence with an external analog filter and HSQC-FF4 recorded with no power for FF sequence without an external analog filter.

oretical value with an error of an order of 7% for $\alpha = 68°$ and 5% for $\alpha = 90°$. Using the HSQC-FF4 experiment all direct ^{13}C, ^{1}H total couplings $T_i^{CH,red}$ could be extracted (Table 4). Thus, $^{1}D_{CH}$ can be derived from Eq. (4) and are in excellent agreement with the back-calculated ones (see Fig. 9) from the crystallographic structure of the (+)-menthol by using the SVD module of the PALES program [23]. A regression factor $R = 0.98$ was obtained for the HSQC-FF4s' using a flip angle of 90° and $R = 0.98$ was calculated by using a flip angle of 68°.

For menthol with its limited spectral range, the FF16-HSQC spectra could also be interpreted despite artefacts. Similar fitting factors R have been found for FF4 and FF16 sequence experiments (results not shown), which is expected also from theory [24] (Fig. 10).

4. Conclusions

We have implemented FF4 decoupling during proton detection for complete removal of homonuclear dipolar couplings. At the same time, the proton chemical shifts as well as heteronuclear couplings are scaled. The simplification and increased dispersion allow extracting C,H dipolar couplings of menthol dissolved in weakly aligning solvents. The FF4-HSQC spectra have a better sensitivity and allow enhancing the resolution by a factor of 1.5–4.2 compared to standard HSQC. FF sequences are very promising for being implemented in other inverse experiments like HMBC or ADEQUATE for measuring long range ^{13}C, ^{1}H and short range ^{13}C, ^{13}C couplings respectively. The results obtained are not limited to small molecules like menthol but could also successfully be applied to more complex compounds with approximately 10 times more protons. We are now exploring the possibility to derive relative stereochemistry of asymmetric centers using FF sequences during detection in experiments for the measurement of homo- and heteronuclear dipolar couplings.

5. Experimental

The liquid–crystalline NMR sample investigated in this work was prepared using a standard procedure. The sample is made of 101 mg of (+)-menthol and 99 mg of PBLG with MW 134,500 that was purchased from Sigma and 426 mg of dry $CDCl_3$, respectively. The concentration of menthol was chosen so high to have excellent signal to noise while optimizing FF-HSQC. Details on the method and sample preparation can be found in literature [25]. All 5 mm O.D. NMR tubes were sealed to avoid solvent

Table 4
Scalar and dipolar couplings of (+)-menthol in PBLG/$CDCl_3$ phase

Atoms couple	J_i^{CH} (±0.5 Hz)	Flip angle (°)					
		68			90		
		$T_i^{CH,red}$ [a] (±0.6 Hz)	T_i^{CH} (±1.2 Hz)	D_i^{CH} [b] (±1.7 Hz)	$T_i^{CH,red}$ [a] (±0.6 Hz)	T_i^{CH} (±1.8 Hz)	D_i^{CH} [b] (±2.3 Hz)
C3–H3	139.1	147.1	280.4	141.3	80.4	259.5	120.4
C4–H4	123.7	157.3	286.0	162.3	88.2	272.8	149.0
C2–H2eq	127.8	83.1	166.2	38.4	62.5	195.4	67.6
C2–H2ax	124.2	139.0	262.3	138.2	82.5	253.0	128.8
C6–H6eq	127.4	113.3	213.8	86.4	74.2	218.3	90.9
C6–H6ax	123.3	158.8	299.6	176.4	97.9	283.7	160.5
C1–H1	123.9	161.8	299.6	175.7	91.8	280.9	157.0
C8–H8	126.2	112.1	211.5	85.2	66.1	213.8	87.6
C5–H5eq	127.8	109.4	210.3	82.5	68.0	219.5	91.7
C5–H5ax	121.4	169.2	307.6	186.1	92.0	292.9	171.5
C7–H7	124.6	119.3	223.9	99.2 (−31.3)	67.9	219.2	94.5 (−29.8)
C9–H9	124.2	37.2	70.1	−54.1 (17.0)	32.5	105.3	−18.9 (5.9)
C10–H10	124.6	61.6	112.0	−12.6 (4.0)	42.8	138.0	13.4 (−4.2)

The uncertainty on C,H couplings and $^{1}D_{CC}$ values are mentioned between brackets. Due to the sufficiently fast rotation of the methyl group about the axis of the carbon to the next heavy atom the $^{1}D_{CH_3}$ depends on the orientation of the vector between the methyl carbon and the directly bound heavy atom. Therefore, the $^{1}D_{CH_3}$ have been turned into $^{1}D_{CC}$ according to $^{1}D_{CC} = {}^{1}D_{CH_3}(-3\gamma_C/\gamma_H)(r_{CH}^3/r_{CC}^3)$, where γ_C and γ_H are the gyromagnetic ratios of carbons and protons and r_{CH}^3 and r_{CC}^3 are the C,H and C,C distances, respectively.

[a] Total spin–spin coupling ($T_i^{CH,red}$) reduced by FF4 scheme.

[b] Deduced dipolar couplings D_i^{CH} [see Eq. (4)].

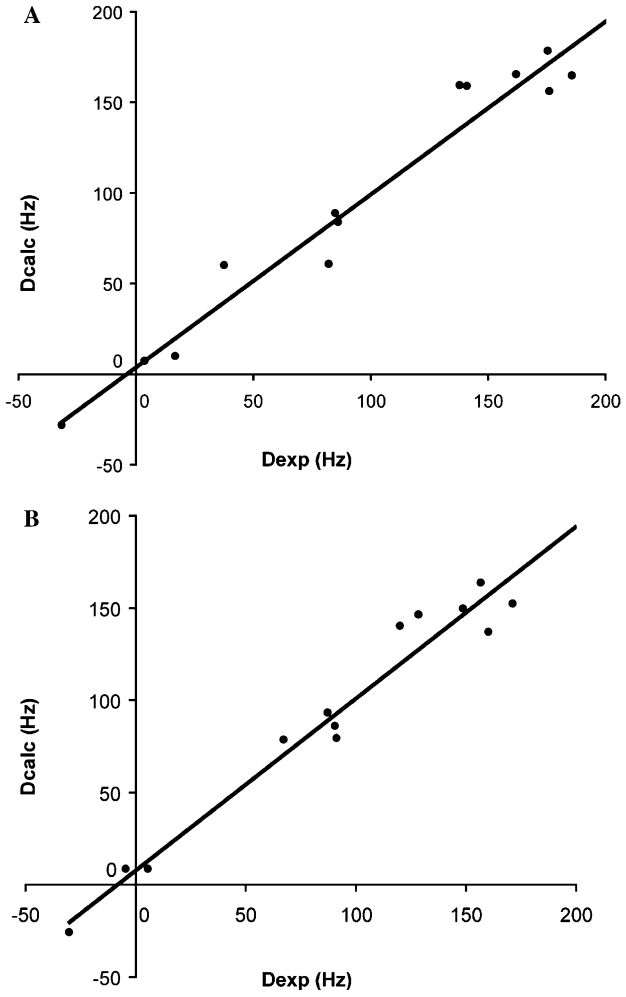

Fig. 9. Correlation between experimental ^{1}H, ^{13}C dipolar couplings ($D_i^{CH,exp}$) extracted from HSQC-FF4 spectra and back-calculated dipolar couplings ($D_i^{CH,calc}$) of (+)-menthol in PBLG/$CDCl_3$. The linear fitting of the 13 $D_i^{CH,exp}$ has the equation $D_{calc} = 0.96 \cdot D_{exp} + 3.76$ for $\alpha = 68°$ (A) and $D_{calc} = 0.93 \cdot D_{exp} + 7.63$ for $\alpha = 90°$ (B). A Pearson factor $R = 0.98$ was obtained for both $\alpha = 68°$ (A), and $\alpha = 90°$ (B).

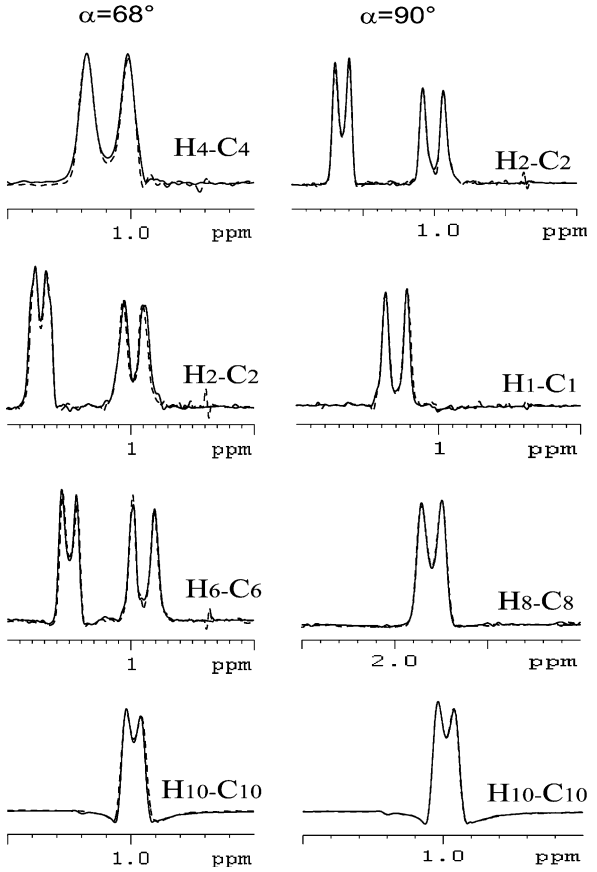

Fig. 10. Superimposition of some F_2-traces for HSQC-FF16 (dotted lines) and HSQC-FF4 (continuous lines). The same acquisition parameters for both experiments were used (see Section 5).

evaporation and centrifuged back and forth until an optically homogeneous birefringent phase was obtained. A quadrupolar splitting of 600 Hz was measured for the deuterium of the solvent that shows the strong alignment of the PBLG phase.

All experiments were carried out on a 900 MHz Bruker Avance spectrometer at 298 K, equipped with a 5-mm triple resonance probe with *xyz* gradients. 1D experiments were acquired with 2k complex data points and 8 scans. To investigate compounds available in small amounts, we have chosen an inverse detection experiment including pulse field gradients for coherences selection as HSQC sequence [26,27] without heteronuclear decoupling during the signal detection to measure direct ^{1}H, ^{13}C couplings. HSQC experiments were recorded with 2048×256 complex data points and 2 scans per experiment. The carrier of all spectra has been set to 1.23 ppm. The spectra were apodized with a $\pi/2$ shifted squared sine-bell function for both dimensions prior to Fourier transform. The final data matrix size after Fourier transform was $4k \times 512$ to ensure a good digital resolution. The digitisation in ω_2 is chosen large to extract dipolar couplings with sufficient accuracy from this dimension. A CYCLOPS phase cycle was implemented on the last 90° (^{1}H) pulse and the receiver to suppress quadrature images in ω_2.

MREV8 and PMLG sequences have been implemented during acquisition but only the FF sequence worked well during acquisition. We implemented the Flip Flop 4 sequence during acquisition by explicit programming. For each block of two pulses (FF2, Fig. 2B), the receiver is blanked when pulses are applied. At the end of FF2, one complex point is sampled. In these conditions, the dwell time is exactly the duration of an FF2 block: $dw = 2\tau'_\lambda + \tau'_\eta + 2t_p$ (see Section 2). We chose to sample points at the end of each FF2 block to have a dwell time value which leads to a spectral width of approximately 10 ppm, i.e., a dwell time $dw = 104.8$ μs corresponding to a spectral width of 9.5 kHz. In these conditions, we have chosen a flip angle of 68° the smallest angle practically usable that leads to a $K_{CS} = 0.51$ for FF4 (Fig. 3A). DR was set to 28% of the dwell time as a compromise between signal reduction due to the blanking/unblanking of the receiver and the efficiency of the decoupling performance.

Theoretically, if the pulses of the FF4 sequence have no power, $E = 1$ and the signal intensity derived from Eq. (5) is reduced to 66% (see Section 2). Experimentally a smaller value has been found, namely 63% that has been calculated as an average value on all proton signals of menthol, compared to normal detection. A flip angle of 90° leading to a $K_{CS} = 0.33$ for the same dw value will also be used for comparison. The FF4 acquisition parameters are reported in the Table 1 for the different flip angles.

No attempts were done to perform the FF4 decoupling using the oversampling (on the Bruker instrument: AQ_mod = DQD) implementation for detection despite the fact that this might be done in a later stage. Instead, we performed the FF decoupling with a simultaneous quadrature (AQ_mod = QSIM) and an analog acquisition mode inducing a noise folding on spectra. The direct effect is the increase in noise of the spectra. Practically this drawback can be avoided by using an external analog filter inserted between the receiver and the analog/digital converter. This filter has been used as a low pass commercially available 4th order butterworth filter with a filter width of 16 kHz.

In our hands, the only reliable way to evaluate the effect of the external analog filter is to compare the signal-to-noise ratio of the FF4 spectra without power in the pulses (with power the noise is not random) recorded with and without analog filter. Indeed, this filter reduced the noise during FF4 decoupling by a factor of 4 (see Table 3 and Fig. 8D).

Acknowledgments

This work has been supported by the Max Planck Society and the Fonds der Chemischen Industrie (to C.G.). It has been on the topic of the DFG-Graduiertenkolleg (GRK 768). J.F. was supported by a Max Planck grant and acknowledges ''Deutscher Akademischer Austausch Dienst'' for a fellowship.

References

[1] (a) A. Annila, P. Permi, Weakly aligned biological macromolecules in dilute aqueous liquid crystals, Concepts Magn. Reson. A 23A (1) (2004) 22–37;
(b) E. de Alba, N. Tjandra, NMR Dipolar couplings for the structure determination of biopolymers in solution, Prog. Nucl. Magn. Reson. Spectrosc. 40 (2002) 175–197.

[2] (a) C. Aroulanda, V. Boucard, F. Guibé, J. Courtieu, D. Merlet, Weakly oriented liquid–crystal NMR solvents as a general tool to determine relative configurations, Chem. Eur. J. (2003) 4536–4539;
(b) L. Verdier, P. Sakhaii, M. Zweckstetter, C. Griesinger, Measurement of long range H,C couplings in natural products in orienting media: a tool for structure elucidation of natural products, J. Magn. Reson. 163 (2003) 353–359;
(c) C. Thiele, S. Berger, Probing the diastereotopicity of methylene protons in strychnine using residual dipolar couplings, Org. Lett. (2003) 705–708.

[3] (a) I. Canet, J. Courtieu, A. Loewenstein, A. Meddour, J.M. Pechine, Enantiomeric analysis in a polypeptide lyotropic liquid–crystal by deuterium NMR, J. Am. Chem. Soc. 117 (24) (1995) 6520–6526;
(b) A. Meddour, P. Berdague, A. Hedli, J. Courtieu, P. Lesot, Proton-decoupled carbon-13 NMR spectroscopy in a lyotropic chiral nematic solvent as an analytical tool for the measurement of the enantiomeric excess, J. Am. Chem. Soc. 119 (1997) 4502.

[4] C. Aroulanda, M. Sarfati, J. Courtieu, P. Lesot, Investigation of the enantioselectivity of three polypeptide liquid–crystalline solvents using NMR spectroscopy, Enantiomer 6 (5) (2001) 281–287.

[5] J.M Lee, W.I. Goldberg, Nuclear magnetic-resonance line narrowing by a rotating rf field, Phys. Rev. A 140 (1965) 1261–1271.

[6] J.S Waugh, L.M. Huber, V. Haeberlen, Approach to high-resolution NMR in solids, Phys. Rev. Lett. 20 (1968) 180.

[7] W.K. Rhim, D.D. Elleman, R.W. Vaughan, Analysis of multiple pulse NMR in solids, J. Chem. Phys. 59 (1973) 3740.

[8] (a) R.G. Pembleton, L.M. Ryan, B.D. Gerstein, NMR probe for combined homonuclear multiple pulse decoupling and magic angle spinning, Rev. Sci. Instrum. 48 (1977) 1286;
(b) L.M. Ryan, R.E. Taylor, A.J. Paff, B.D. Gerstein, Experimental-study of resolution of proton chemical-shifts in solids—combined multiple pulse NMR and magic-angle spinning, J. Chem. Phys. 72 (1980) 508.

[9] D.P. Burum, W.K. Rhim, W. K, Analysis of multiple pulse NMR in solids, J. Chem. Phys. 71 (1979) 944.

[10] D.P. Burum, N. Linder, R.R. Ernst, Low-power multipulse line narrowing in solid-state, NMR J. Magn. Reson. 44 (1981) 173.

[11] B.M. Fung, A comparison of homonuclear dipolar-decoupling techniques in heteronuclear experiments, J. Magn. Reson. 72 (1987) 353.

[12] A. Bielecki, A.C. Kolbert, M.H. Levitt, Frequency-switched pulse sequences—homonuclear decoupling and dilute spin NMR in solids, Chem. Phys. Lett. 155 (1989) 341.

[13] P. Jensen, H.J. Sass, S. Grzesiek, Improved detection of long-range residual dipolar couplings in weakly aligned samples by Lee–Goldburg decoupling of homonuclear dipolar truncation, J. Biomol. NMR 30 (2004) 443–450.

[14] (a) J.M. Ouvrard, B.N. Ouvrard, J. Courtieu, C.L. Mayne, D.M. Grant, Coherent reduction of dipolar interactions in molecules dissolved in liquid–crystal solvents using a new multiple-pulse technique during acquisition, J. Magn. Reson. 93 (1991) 224–241;
(b) P. Lesot, J.M. Ouvrard, B.N. Ouvrard, J. Courtieu, Coherent reduction of dipolar interactions in molecules dissolved in anisotropic media using a new multiple-pulse sequence in a COSY experiment, J. Magn. Reson. A. 107 (1994) 141–150;
(c) P. Lesot, F. Nielsen, J.M. Ouvrard, J. Courtieu, Multiple-pulse COSY NMR-spectroscopy of oriented molecules in thermotropic cholesterics, J. Phys. Chem. 98 (1994) 12849–12855;
(d) P. Lesot, J.W. Emsley, J.M. Ouvrard, E. Curzon, Simplification of F-19 NMR spectra of liquid crystalline samples by multiple-pulse COSY experiments, J. Magn. Reson. 133 (1998) 166–172.

[15] J. Courtieu, J.P. Bayle, B.M. Fung, Variable angle sample spinning in liquid crystals, Prog. Nucl. Reson. Spectrosc. 26 (1994) 141–1653.

[16] M.C. Thiele, Scaling the alignment of small organic molecules in substituted polyglutamates by variable-angle sample spinning, Angew. Chem. Int. Ed. 44 (2005) 2–5.

[17] J. Farjon, D. Merlet, P. Lesot, J. Courtieu, Enantiomeric excess measurements in weakly oriented chiral liquid crystal solvents through 2D H-1 selective refocusing experiments, J. Magn. Reson. 158 (2002) 169–172.

[18] J. Farjon, J.P. Baltaze, P. Lesot, D. Merlet, J. Courtieu, Heteronuclear selective refocusing 2D NMR experiments for the spectral analysis of enantiomers in chiral oriented solvents, J. Magn. Reson. Chem. 42 (2004) 594–599.

[19] C.W. Vander Kooi, E. Kupce, E.R.P. Zuiderweg, M. Pellecchia, Line narrowing in spectra of proteins dissolved in a dilute liquid crystalline phase by band-selective adiabatic decoupling: Application to H-1(N)-N-15 residual dipolar coupling measurements, J. Biomol. NMR 15 (1999) 335–338.

[20] V. Chevelkov, Z. Chen, W. Bermel, B. Reif, Resolution enhancement in MAS solid-state NMR by application of C-13 homonuclear scalar decoupling during acquisition, J. Magn. Reson. 172 (2004) 56–62.

[21] K. Fehér, S. Berger, K.E. Kovér, Accurate determination of small one bond heteronuclear residual dipolar couplings by F1 coupled HSQC modified with a GBIRD(r) module, J. Magn. Reson. 163 (2003) 316–340.
[22] J.M. Ouvrard, Simulation of 1D and 2D NMR by using the Matrix density Formalism. Application to the Coherent Reduction of the Spin Hamiltonian, Ph.D. Thesis, University of Paris Sud, Orsay, France, 1990.
[23] M. Zweckstetter, A. Bax, Prediction of sterically induced alignment in a dilute liquid crystalline phase: aid to protein structure determination by NMR, J. Am. Chem. Soc. 122 (2000) 3791–3792.
[24] P. Lesot, Developments and Applications of New NMR Methodologies in Liquid Crystal Media, Ph.D. Thesis, University of Paris Sud, Orsay, France, 1995.
[25] M. Jakubcova, A. Meddour, J.M. Pechine, A. Baklouti, J. Courtieu, Measurement of the optical purity of fluorinated compounds using proton decoupled F-19 NMR spectroscopy in a chiral liquid crystal solvent, J. Fluorine Chem. 86 (1997) 149–153.
[26] G. Bodenhausen, D.J. Ruben, natural abundance N-15 NMR by enhanced heteronuclear spectroscopy, Chem. Phys. Lett. 69 (1980) 185–189.
[27] (a) A.L. Davis, E.D. Laue, J. Keeler, D. Moskau, J. Lohman, Absorption-mode two-dimensional NMR-spectra recorded with pulsed field gradients, J. Magn. Reson. 94 (1991) 637–644;
(b) A.L. Davis, J. Keeler, D. Moskau, Experiments for recording pure absorption heteronuclear correlation spectra using pulsed field gradients, J. Magn. Reson. 98 (1992) 207–216.